Chemical Engineering Science 71 (2012) 202–211

Contents lists available at SciVerse ScienceDirect

Chemical Engineering Science

journal homepage: www.elsevier.com/locate/ces

Modeling the effect of blood viscosity on hemodynamic factors in a small bifurcated artery

A.G. Kanaris, A.D. Anastasiou, S.V. Paras *

Laboratory of Chemical Process and Plant Design, Department of Chemical Engineering, Aristotle University of Thessaloniki, Greece

ARTICLE INFO

Article history:
Received 26 September 2011
Received in revised form
8 December 2011
Accepted 13 December 2011
Available online 19 December 2011

Keywords:
Hematocrit
Viscosity
Wall shear stress
Hypertension
Small artery
CFD

ABSTRACT

Many studies link hyperviscosity to cardiovascular diseases, hypertension and cerebral infraction, rendering the study of hemodynamic factors very important for understanding, predicting and treating this type of disorders. In this work the effect of blood viscosity on several hemodynamic factors, such as wall shear stress (*WSS*), wall shear stress gradient (*WSSG*), blood flow rate and pressure drop in a small-caliber bifurcated artery (parent: 600 μm, daughters: 470 μm) was numerically studied. A *CFD* code, validated by relevant experimental data acquired in this Lab, was used for the simulations. In order to simulate the pulsatile flow of blood a velocity fluctuation has been imposed (U_{mean}=0.080–0.105 m/s) as inlet boundary condition. As blood is a non-Newtonian fluid, its viscosity was calculated using the *Casson* model. The results showed that, when blood viscosity increases, the heart must also increase its pumping power (up to 126%) in order to keep cardiac output unchanged. On the other hand, and if it is assumed that the pumping power of the heart is fixed, the blood flow rate is attenuated accordingly (by 64% for the highest hematocrit studied). For all cases studied it was found that at the outer wall of the bifurcation *WSS* values are lower than those on the rest of the arterial wall. The high *WSS* and *WSSG* values calculated at the apex of the bifurcation (10 Pa and 4×10^4 Pa/m, respectively, for H_t=45%) indicate that this location is predisposed to endothelium damages. These findings could aid in the comprehension of the mechanisms related to vascular damages caused by hyperviscosity.

1. Introduction

The human circulatory system is a well-designed and perfectly controlled pumping system. It consists of two fluid pumps in series, (i.e. the left and the right heart ventricle), and a complicated, branched pipeline network (i.e. large arteries, small arteries, arterioles, capillaries and veins) (e.g. Kroemer et al., 2010). A key factor for the normal operation of this system is the *viscosity* of the blood, which describes the resistance to flow and determines the pressure drop and the wall shear stress (*WSS*).

Blood viscosity can be affected by various factors (e.g. hemospherine, glucose, proteins) the most important of them being hematocrit (H_t), which denotes the percentage of blood volume that is occupied by red blood cells. In healthy individuals moderate variations in hematocrit and therefore blood viscosity can often occur (Salazar-Vazquez et al., 2006) without affecting their health provided that the advanced compensation mechanisms of human organism work properly. In human circulatory system the endothelium acts as a sensor, which detects viscosity variations through the changes in wall shear stress (*WSS*). Consequently, vasoactive materials, such as nitric oxide (*NO*), prostacyclin and endothelin, are produced. These compounds can reduce the resistance to flow and maintain blood circulation by affecting the microvascular diameter (John, 2009). The effect of the aforementioned compensation mechanisms can be reduced when blood exhibits high hematocrit values (i.e. hyperviscosity) (Salazar-Vazquez et al., 2006).

In a blood vessel with stable lumen diameter an increased viscosity would lead to higher than normal *WSS* values. According to Malek et al. (1999) *WSS* values in a healthy artery are in the range of 1–7 Pa. In large vessels, the chronic exposure of the endothelial surface to greater than normal *WSS* values could lead to thrombosis and further damage of the endothelium (Fig. 1). On the other hand, in small vessels hyperviscosity can lead to a reduction of blood flow and therefore to lower *WSS* values (in the range of 0.4 Pa), which in turn can promote the development of atherosclerosis (Chatzizisis and Giannoglou, 2006). Another factor that affects endothelial proliferation is the spatial wall shear stress gradient (*WSSG*), a hemodynamic index that represents the spatial non-uniformity of *WSS* (Dolan et al., 2011). It is reported that this non-uniformity of hemodynamic forces may

* Correspondence to: Laboratory of Chemical Process and Plant Design, Department of Chemical Engineering, Aristotle University of Thessaloniki, University Box 455, GR 54124 Thessaloniki, Greece. Tel.: +30 2310 996174; fax: +30 2310 996209.
E-mail address: paras@auth.gr (S.V. Paras).
URL: http://philon.cheng.auth.gr (S.V. Paras).

0009-2509/$ - see front matter © 2011 Elsevier Ltd. All rights reserved.
doi:10.1016/j.ces.2011.12.015

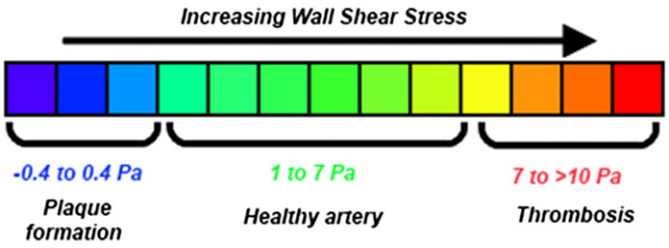

Fig. 1. Variation of Wall Shear Stress (*WSS*) in humans.

affect biological processes in endothelial cells (Shimogonya et al., 2009). In a local coordinate system *WSSG* is given by

$$WSSG = \sqrt{\left(\frac{\partial WSS_m}{\partial m}\right)^2 + \left(\frac{\partial WSS_n}{\partial n}\right)^2} \quad (1)$$

where m is the direction of the *WSS* vector and n is the direction normal to m and tangential to the arterial surface (Murphy and Boyle, 2010). Tissue growth has been reported to occur in areas where *WSS* has a low while *WSSG* has a high value (Farmakis et al., 2004; Murphy and Boyle, 2010). In order to find indications of possible problematic areas, *WSS* must be examined in conjunction with *WSSG*.

Dolan et al. (2011) discuss the combined effect of *WSS* and *WSSG* on the endothelial cells. By conducting well designed *in vitro* experiments, they investigated the way the endothelium responses to a range of elevated *WSS* in conjunction with positive or negative *WSSG* values. They report that the response of the endothelial cells to high *WSS* and *WSSG* have potentially important biological implications.

Numerous clinical and epidemiological studies have related hyperviscosity to hypertension, decreased flow rate and more generally to pathogenesis of many cardiovascular diseases. It is also known that diabetic patients show a significant reduction in capillary blood cell velocities in comparison with normal subjects and that both diabetes and atherosclerosis cause occlusions of the oxygen-transporting vessels, thus leading to tissue ischemia and necrosis. Cuypers et al. (2000), who conducted clinical experiments, report a negative correlation between blood glucose level and blood flow rate. Salazar-Vazquez et al. (2006), who investigated the effect of hematocrit on blood pressure in diabetic patients, state that high hematocrit values ($H_t > 43\%$) can be associated with hypertension. Works published by Lowe et al. (1997) and Woodward et al. (2003) report that blood viscosity can be considered a risk factor for cardiovascular diseases, having the same importance as *LDL* cholesterol and smoking. Tohgi et al. (1978) report that the risk of cerebral infraction increases remarkably when hematocrit values exceed 45%. It is also stated (Stack and Berger, 2009) that many athletes who made use of human erythroprotein (blood "doping") died suddenly of heart attack due to the high viscosity of blood and the reduction of its flow rate.

Given the above, the importance of **blood viscosity** for the normal operation of the human circulatory system can be readily deduced. In order to develop new methods for predicting and treating cardiovascular diseases, it would be useful to quantify the effect of blood viscosity on pressure drop, *WSS* and blood flow rate in small caliber arteries. To the authors' best knowledge, little work has been published on this subject. Çinar et al. (1999) comment on the effect of hematocrit on viscosity and consequently on related changes in blood pressure, velocity and lumen diameter. However their results are questionable, since they are based on the simplified assumption that blood exhibits Newtonian behavior, a fact that holds true only for large diameter arteries, where shear rate values are greater than 1000. Stack and Berger (2009) published a phenomenological study on the physiological effects of increased hematocrit, for a small and straight artery (1 mm in diameter). Their work focuses on the form of the velocity profiles for various hematocrit values (H_t=40-80%). As a conclusion, none of the aforementioned studies investigates explicitly the effect of blood viscosity on *WSS*.

Numerous investigations indicate curvatures and bifurcations of large and medium sized arteries to be high risk regions for cardiovascular diseases (Perktold and Rappitsch, 1994). In such areas of the arterial tree dramatic hemodynamic alternations can occur due to secondary flows resulting from the combination of centrifugal and viscous forces. These regions are characterized by low local *WSS*, which affect the generation and the progression rate of atherosclerosis (e.g. Shaaban and Duerinckx, 2000; Chatzizisis and Giannoglou, 2006).

Given the above, the **scope** of this work is to quantify the effect of increased viscosity, on important hemodynamic factors such as pressure drop, *WSS*, *WSSG* and blood flow rate in a small-caliber **bifurcated** artery. Instead of elaborated *in vivo* experiments, the flow is simulated using a well-established and validated *CFD* code. The results of this study will allow better insight on the effect of viscosity changes on the function of arteries of this size and consequently on the human circulatory system.

2. Computational procedure

2.1. Blood viscosity model

It is known that blood is a multiphase mixture of plasma, a Newtonian fluid, and three main cell types, namely red blood cells, platelets and leukocytes. Due to its composition blood has a significantly ***non-Newtonian*** behavior (Truskey et al., 2004). At very low shear rate values normal red cells form linear aggregates (*rouleaux*), which disrupt flow streamlines and greatly increase the apparent blood viscosity. By increasing the shear rate, these aggregates are progressively deformed and consequently the apparent viscosity decreases to an asymptotic value. However, for flow in large arteries blood can be considered a continuous fluid, whose behavior can be adequately described in terms of bulk properties. On the other hand, when the diameter of the blood vessels is comparable to that of the red blood cells, the aforementioned assumption does not hold true. In such small vessels red blood cells drift to the central axis of the vessel and a cell-free layer, called a plasma layer, is formed along the vascular wall. As a result the apparent blood viscosity declines substantially with decreasing diameter, a behavior known as the *Fahraeus–Lindqvist* effect (Pries et al., 1990). This effect becomes more significant for blood vessels with diameter smaller than 300 μm.

Many models have been developed to describe blood viscosity, the most widely used of which is the *Casson* model (Neofytou, 2004).

$$\sqrt{\tau} = \sqrt{\tau_y} + \sqrt{n_N \gamma} \quad (2)$$

where τ is the shear stress, γ the shear rate, τ_y the yield stress and n_N the blood viscosity for high shear rates (asymptotic value). The yield stress is a measure of the energy required for breaking down the aggregates of red blood cells formed at very low shear rates. Merrill (1969), who extensively investigated blood rheology, confirms the strong relation between viscosity and hematocrit and suggests the terms n_N and τ_y of Eq. (2) to be expressed as functions of hematocrit, i.e.

$$n_N = n_p[1 + 0.025H_t + 7.35 \times 10^{-4} H_t^2] \quad (3)$$

where n_p is the viscosity of the plasma

$$\tau_y = A(H_t - H_c)^3 \quad (4)$$

and H_c is the critical hematocrit, below which the yield stress, τ_y, can be considered negligible. For normal blood H_c ranges between 4 and 8 and A is a constant ranging between 0.6×10^{-7} and 1.2×10^{-7} Pa. The aforementioned expressions are employed hereafter for predicting blood viscosity as a function of hematocrit (Fig. 2). In Table 1 the parameters of the *Casson* model are given for five hematocrit values.

For the sake of simplicity the variations in viscosity, which, as already mentioned, can be attributed to several factors, are expressed in the simulations as a function of hematocrit alone. Blood density, ρ, is assumed to be constant, i.e. independent of the hematocrit value investigated, and equal to 1050 kg/m^3.

2.2. CFD code validation

The commercial *CFD* code *ANSYS CFX*® 13.0 was employed for the simulations, for solving the incompressible Navier–Stokes equation. The reliability of the code was tested by comparing its results with relevant experimental data acquired in this Lab (Anastasiou et al., in press). Several images acquired by a camera through a microscope at various channel depths were used for constructing a model of the microchannel using *CAD* software (*ANSYS Workbench*). The geometry and the dimensions of the bifurcated channel are shown in Fig. 3. It should be noted that, due to manufacturing reasons, the mother and daughter branches are of the same caliber. The *blood analogue* fluid used for the experiments is defined in the *CFD* code preprocessor as a non-Newtonian liquid, whose viscosity follows the *Casson* model (Fig. 4). Since the flow is symmetric with

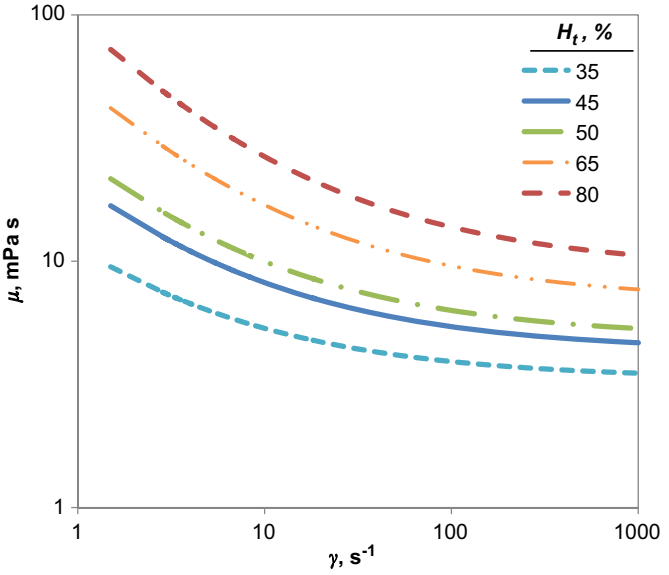

Fig. 2. Blood viscosity for various hematocrit values predicted by the *Casson* model.

Table 1
Parameters of the *Casson* model for various hematocrit values.

Hematocrit (%)	τ_y *(Pa)*	n_N *(Pa s)*
15	0.00	0.018
35	0.02	0.031
45	0.06	0.043
50	0.09	0.049
80	0.45	0.092

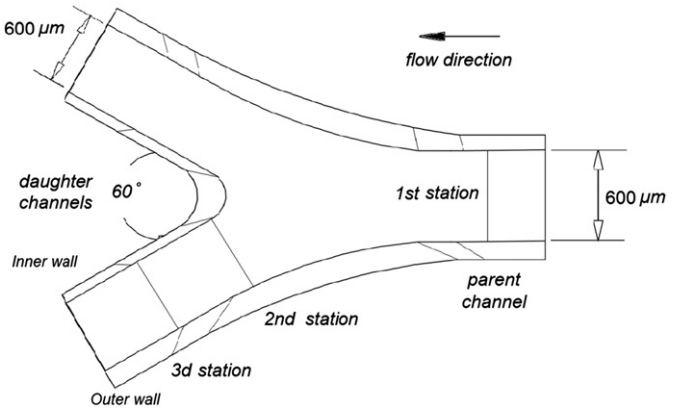

Fig. 3. Geometry and dimensions of the bifurcation employed in the experiments (Anastasiou et al., in press).

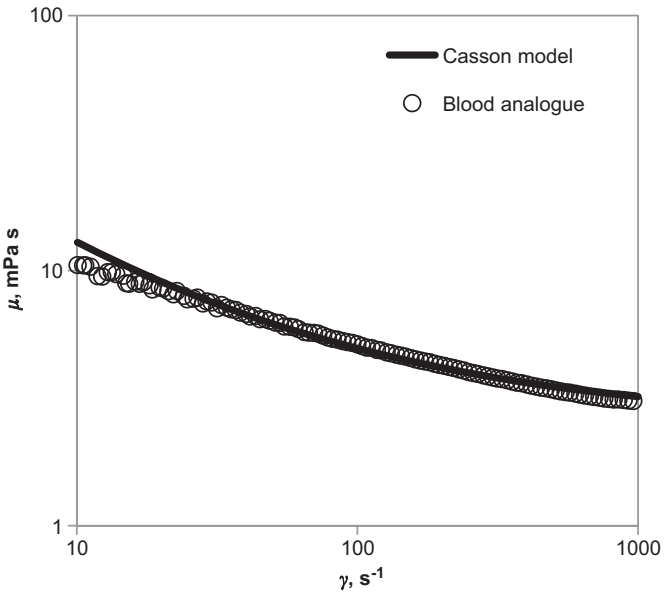

Fig. 4. Fitting of the blood analog viscosity by the *Casson* model.

respect to the middle plane and in order to minimize *CPU* time and computational power needed, it is considered sufficient to perform the calculations only in one daughter tube and the corresponding part of the parent tube.

As the accuracy of the solution strongly depends on the number and the size of the cells, a grid dependence study was performed to select the appropriate mesh density for the *CFD* model. The grids tested were unstructured, comprising both tetrahedral and prism elements. The results of velocity distribution at the bifurcation (for $Re=17$–21) were compared for four different mesh densities, ranging from 0.8 to 3 million elements. The grid selected for the simulations comprises about 950,000 tetrahedral and prism elements of maximum element edge size up to 15 μm. Special treatment has been applied near the area of the bifurcation apex in terms of grid density and quality.

As the experiments were conducted under pulsatile-flow conditions the solution is time-dependant and hence the simulations were run in ***transient*** mode. A timestep-dependence study was also performed, to ensure that a suitable timestep duration is selected. Finally, a timestep of 0.05 s (leading to 20 time-steps) was chosen as the optimum, i.e. the minimum number of calculation steps performed without jeopardizing the accuracy of the solution. The pulsatile flow conditions applied during the

experiments was mathematically described by a 6th order polynomial, which is fitted to the experimental velocity data at the parent tube entrance and was used as an inlet boundary condition (Fig. 5a). The pulse used for the simulation can be considered typical for small-caliber arteries (Kroemer et al., 2010).

Since *Reynolds* number is low (laminar flow conditions) Direct Numerical Simulation (*DNS*) was applied for the simulations. Due to the increased computational demand of the numerous simulations a high performance cluster (*HPC*) for parallel computation (available in our Lab), consisting of 24 cores and 64 GB RAM, was used.

The simulation results were found to be in very good agreement with experimental data concerning both velocity profiles (Fig. 6a and b) and *WSS* (Fig. 6c). It is therefore suggested that the use of the *Casson* model for simulating blood viscosity in conjunction with the application of *in vivo* flow conditions (i.e. pulsatile flow) lead to reliable results. Therefore, *CFD* modeling can be considered a dependable tool for studying blood flow characteristics in small arteries.

2.3. Modeling of blood flow in a small-caliber bifurcated artery

Following the successful validation of the code, a small-caliber bifurcated artery of cylindrical shape was considered a realistic model (Fig. 7a). The parent artery has similar dimensions to the

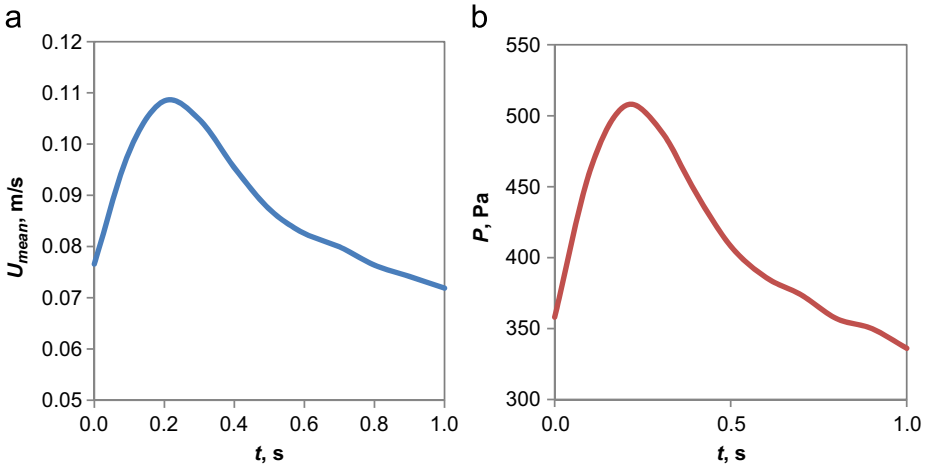

Fig. 5. Boundary conditions imposed at the inlet of the parent channel: (a) velocity fluctuations for *case A* and (b) pressure fluctuations for *case B*.

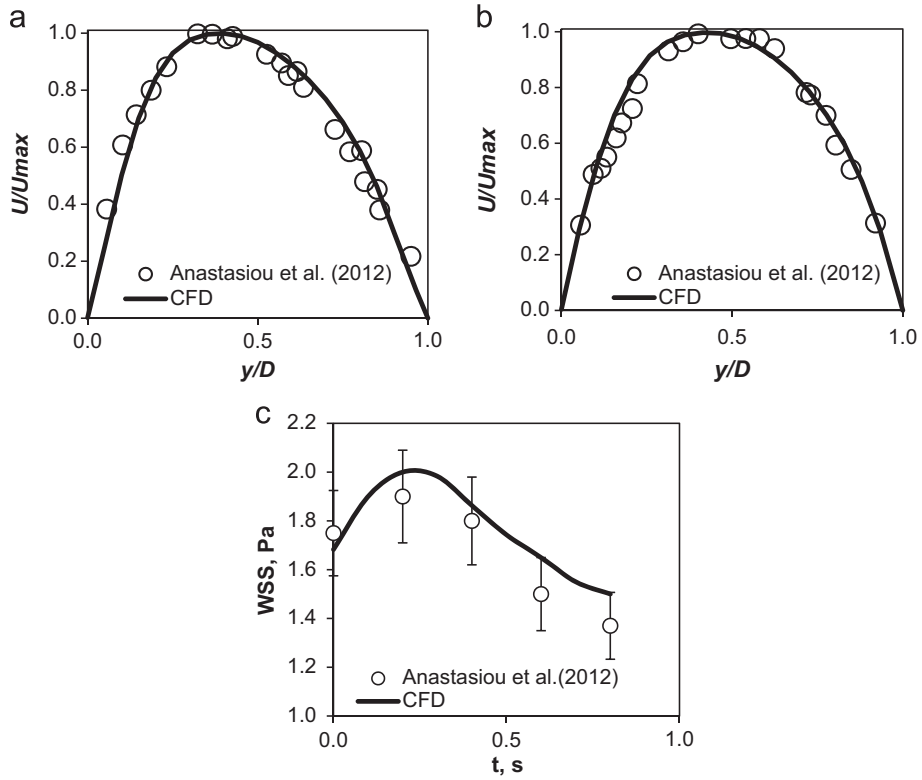

Fig. 6. Comparison of *CFD* code results with the experimental data, at station 2, for the normalized velocity on: (a) the minimum and (b) the maximum of the inlet pulse and (c) *WSS* (5% error bars).

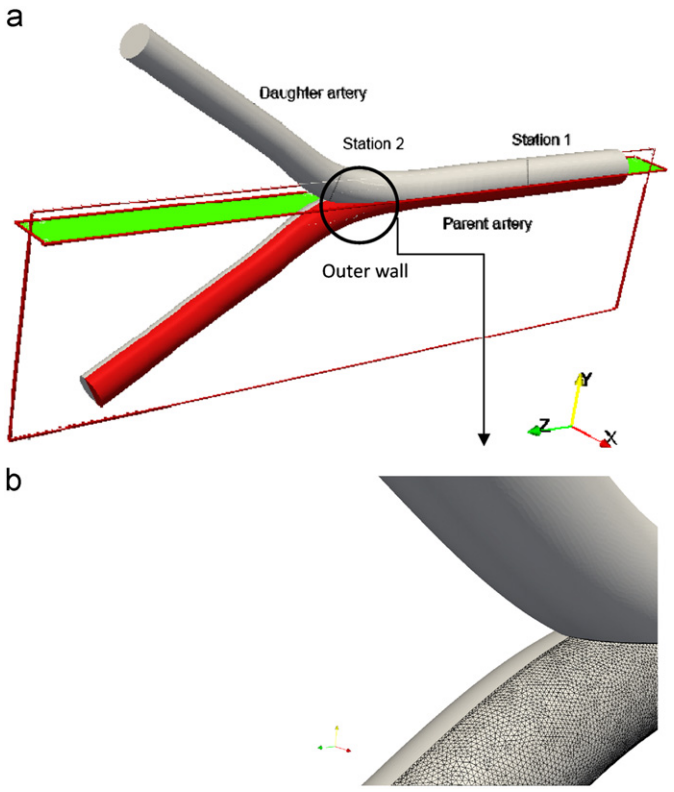

Fig. 7. (a) Geometry of the bifurcated artery used for numerical simulations and (b) detail of the grid used.

one used for validating the code, i.e. a hydraulic diameter of 600 μm and a typical angle of 60°, while the diameters of the daughter arteries are calculated using the Murray law (Eq. (5)) (Murray, 1926).

$$D^3 = D_1^3 + D_2^3 \tag{5}$$

where D is the diameter of the parent artery and D_1 and D_2 are the diameters of the daughter arteries. In this case the two daughter arteries are assumed identical and hence $D_1 = D_2 = 474$ μm. The Murray law is widely used for determining the dimensions of branching (e.g. Yang et al., 2007; Olufsen et al., 2000). It must be noted that blood viscosity is regarded independent of the conduit diameter (*Fahraeus–Lindqvist* effect), since the diameter of the conduits employed are greater than 300 μm.

The model of the bifurcated artery was designed in *Autodesk AutoCAD®* and was imported in the meshing application of the *CFD* code. As the model has two planes of symmetry, i.e. one parallel (*plane YZ*) and one perpendicular (*plane XZ*) to the bifurcation (Fig. 7a), by meshing only part of the geometry, the computational burden is considerably reduced. A grid dependence study was also performed for this geometry and the minimum number of necessary elements is found to be approx. 2 million. A detail of the grid is presented in Fig. 7b.

Pulsatile blood flow simulations were performed using the validated *CFD* code. The vessel walls are assumed rigid, since in these small arteries the wall elasticity can be considered negligible. The no-slip condition was applied to the vessel walls, while a constant pressure boundary condition (relative pressure, $P = 0$ Pa) was set at the model outlet. In order to investigate the effect of viscosity on blood flow characteristics, simulations were conducted for a set of hematocrit values (i.e. 35%, 45%, 50%, 65%, 80%) that correspond to a wide range of viscosity values, i.e. from normal to hyperviscosity. Two cases were considered, namely ***case A*** and ***case B***.

- In ***case A*** the inlet velocity is a pulse (i.e. a temporal function) whose characteristic parameters (frequency, amplitude) are considered constant (Fig. 5a), i.e. $f = 1$ Hz and $U_{mean} = 0.080$–0.105 m/s. In this case, it is assumed that the heart produces the necessary pumping power for maintaining the required blood flow. The inlet velocity values follow the previously mentioned 6th order polynomial, allowing the study of the effect of different hematocrit values on blood pressure, *WSS* and *WSSG*.
- In ***case B*** it was assumed that the heart is for some reason unable to increase its pumping power above a certain value. Thus, when the viscosity, or equally the hematocrit, is increased the heart can overcome the resulting resistance to flow, i.e. the pressure drop, only by reducing the blood flow rate. This scenario is realized by imposing as inlet boundary condition a pressure fluctuation that corresponds to a typical inlet velocity pulse (for $H_t = 45\%$), which is calculated using data from *case A* (Fig. 5b). Thereupon the **same** pressure function was used as inlet boundary condition for all simulations, allowing the study of mass-flow change due to the change in blood viscosity.

The calculations were performed using double-precision variables, while the high resolution advection scheme was used to avoid the diffusive discretization errors of commonly used upwind differencing scheme. The second order backward Euler transient scheme is also employed to avoid similar problems with numerical diffusion (ANSYS Inc., 2011). All simulations were performed until the convergence criterion is met (i.e. mass residuals less than 10^{-8}). Direct Numerical Simulation (*DNS*) was applied for all cases since *Re* values are lower than 30 (laminar flow).

3. Results and discussion

Axial velocity profiles are calculated at *stations 1* and *2* located at the parent artery and at the entrance of the bifurcation, respectively (Fig. 7a). *WSS* values are calculated by the *CFD* code, while *WSSG* values are computed at each node using the open source post-processing software *Kitware Paraview 3.10.1* (Kitware Inc., 2011).

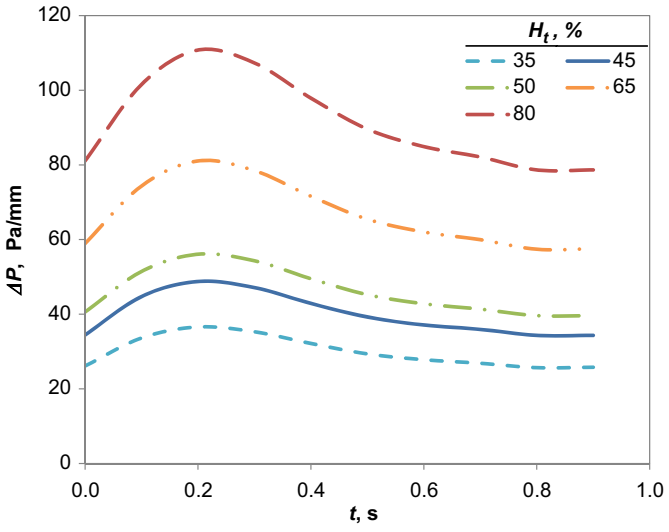

Fig. 8. Pressure drop for various hematocrit values (*case A*).

In Fig. 8 the pressure drop during a pulse cycle is presented for ***case A***. In this case the pressure drop is indicative of the energy that the heart must produce to maintain the blood flow, assuming that the compensation mechanisms are ineffective. The curve corresponding to H_t=45% is considered to be the normal condition and used as reference. It is evident that the pressure drop is proportional to hematocrit and consequently to blood viscosity. An increase of the hematocrit by 11% (i.e. from 45% to 50%) leads to an increase of the asymptotic viscosity by 14% (from 4.3 to 4.9) and consequently to a 14% increase of the pressure drop. For H_t=80% the asymptotic viscosity values increase by 110% (from 4.3 to 9.2), which results to a 126% pressure drop increase.

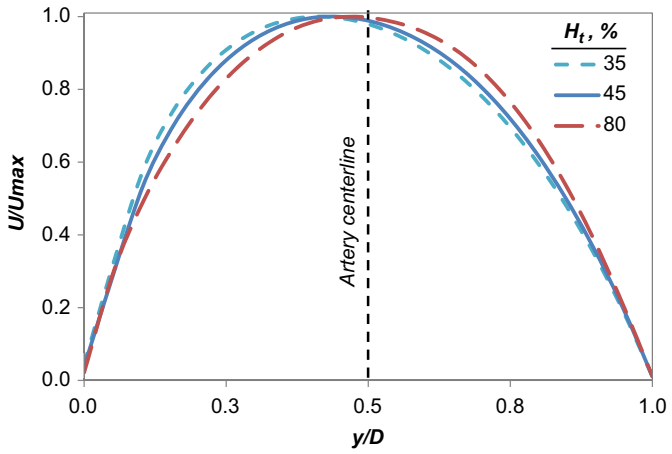

Fig. 9. Normalized axial velocity profiles for the two extreme and the normal hematocrit values at station 2 (*case A*).

It is well known that the flow in bifurcated vessels is characterized by the skewing of velocity profile towards the inner wall due to the centrifugal forces. In Fig. 9 the axial velocity profiles at *station 2*, normalized with respect to the maximum velocity, for the two extreme (35% and 80%) and the normal hematocrit values (45%) are presented. For H_t=35% this skewing is more intense, since for this hematocrit the viscosity attains its lowest value. On the other hand, for H_t=80% (the highest viscosity employed) the velocity retains its parabolic profile. This change of the velocity profile shape has a direct effect on the local *WSS* values. It was found that for H_t=35% the *WSS* value on the inner wall is 64% greater than that on the outer wall. This difference rises to 52% for H_t=45% and 36% for H_t=80%. For all cases studied velocity returns to its normal parabolic profile one diameter downstream from the bifurcation. This was also verified by Anastasiou et al. (in press), who performed relevant experiments.

The variation of *WSS* with blood viscosity was also investigated for ***case A***. In Figs. 10–12 *WSS* values are shown at the pulse peak (i.e. t=0.2 s) and for hematocrit values 45%, 65% and 80%, respectively. For H_t=45% it is clear that *WSS* values are not greater than 7 Pa at the parent artery (Fig. 10a), a fact that, according to Fig. 1, denotes a healthy condition. However, on the

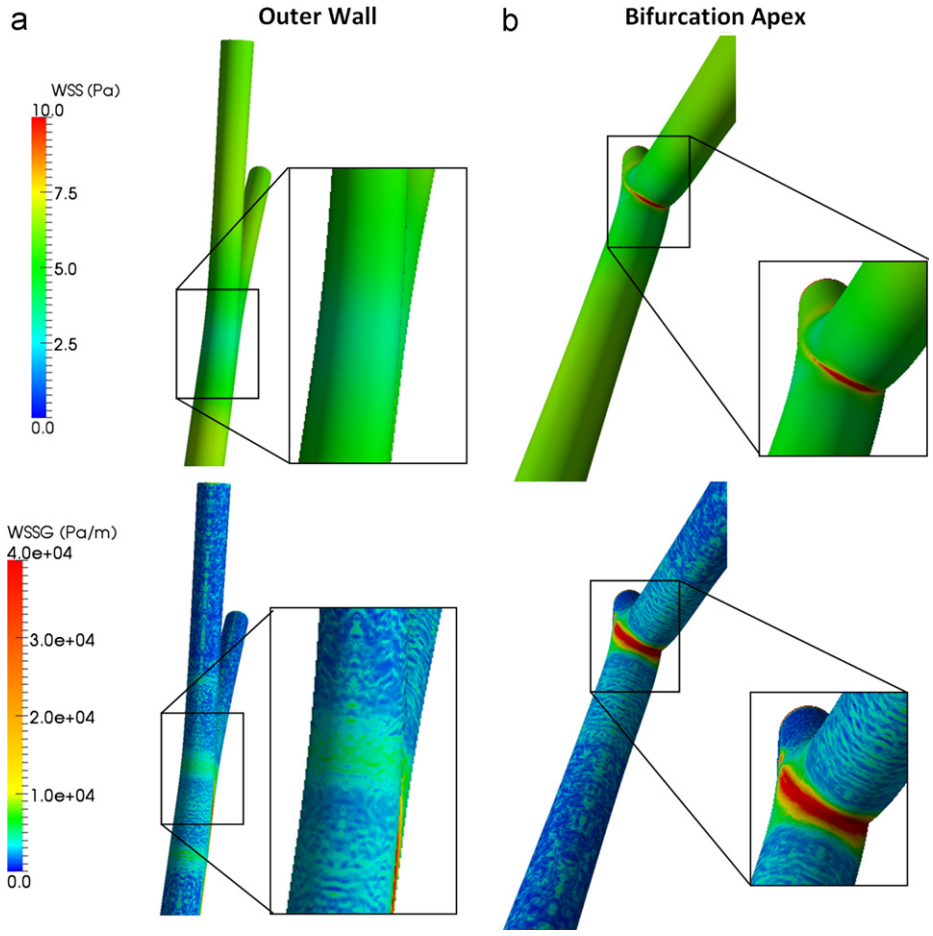

Fig. 10. WSS and WSSG on (a) the outer wall and (b) the apex of the bifurcation, for H_t=45% (*case A*, t=0.2 s).

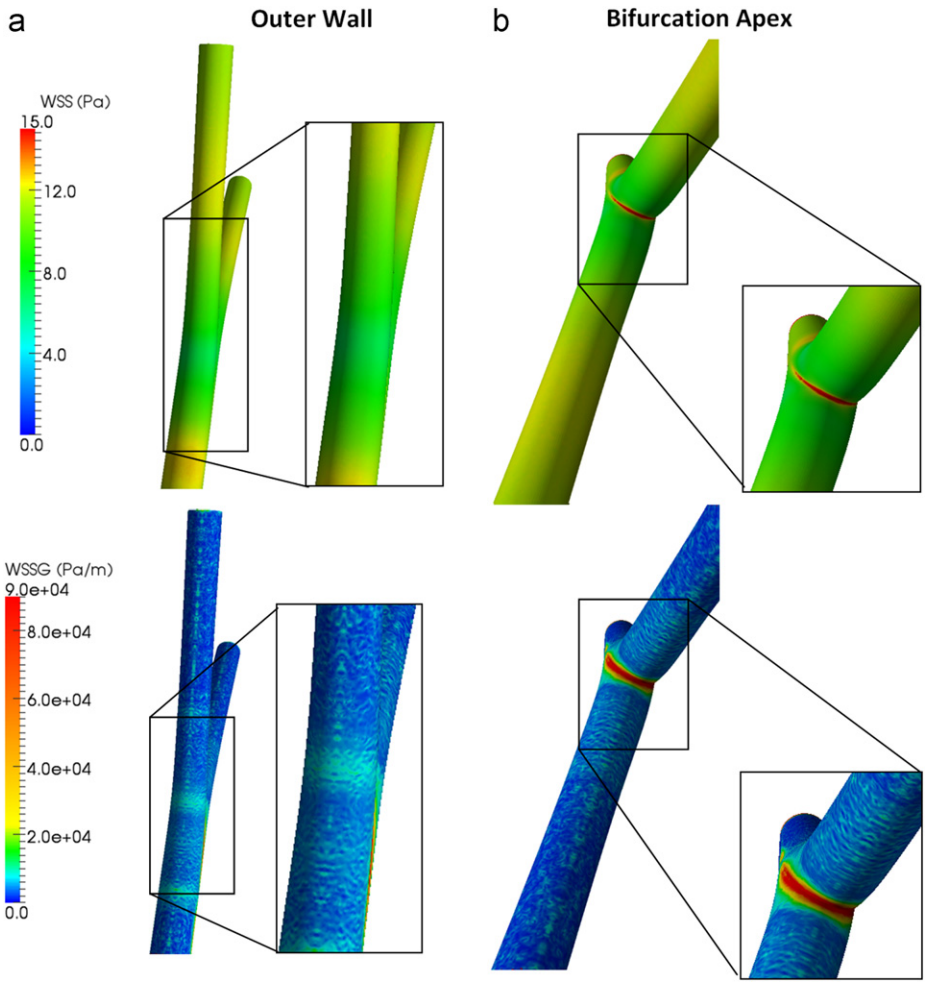

Fig. 11. *WSS* and *WSSG* on (a) the outer wall and (b) the apex of the bifurcation, for H_t=65% (*case A*, t=0.2 s).

outer wall of the bifurcation *WSS* is lower than 3 Pa, while at the same area *WSSG* is about 7000 Pa/m. This combination indicates a *high-risk* zone for atherosclerotic plaque formation, since the exposure of the endothelial cells to low *WSS* and high *WSSG* alters the transendothelial permeability and promotes migration and cell loss (Phelps and DePaola, 2000). If the hematocrit value is increased from 45% to 65% (Fig. 11a), corresponding to a viscosity increase from 4.3 to 6.9 mPa s, *WSS* values at the straight parts of the artery are also increased to 11.5 Pa, while for H_t=80% *WSS* exceeds 14.5 Pa (Fig. 12a). These elevated values are associated with the risk of thrombosis and endothelium cell damage. However, at the outer wall of the bifurcation, *WSS* is lower compared with this at the straight parts of the artery but not low enough to promote atherosclerosis (i.e. greater than 3 Pa) even for high viscosity.

On the other hand, at the ***bifurcation apex*** (i.e. the junction between the two daughter arteries) both *WSS* and *WSSG* values are particularly increased. As it is apparent, *WSS* on the bifurcation apex is taking very high values compared to the rest of the artery walls regardless of the hematocrit. While for H_t=45% *WSS* is not greater than 9.5 Pa (Fig. 10b), it increases up to 14.5 Pa (Fig. 11b) and 27 Pa (Fig. 12b), for *Ht*=65% and 80%, respectively. It is known (Dolan et al., 2011) that this area exhibits elevated *WSS* and *WSSG* values and that 28 Pa is a value for *WSS* that often encountered near the apices of bifurcations. It is reported that this condition has a negative effect on the endothelial alignment (leading to apoptosis) and reduces cell density. As H_t (or equally viscosity) is increased, these areas of high *WSS* and *WSSG* are enlarged and consequently the risk of endothelial cell dysfunction is increased. It should be noted that although the very high values of *WSSG* may be attributed to the sharp edges of the computational geometry used, the qualitative results regarding the *WSSG* remain useful for predicting high-risk zones in conjunction with *WSS* values.

Of great interest are the results of ***case B,*** where a given pumping power is assumed to be produced by the heart (i.e. corresponding to H_t=45%). In Fig. 13 the blood mass flow rate for a full pulse cycle for hematocrit values 45%, 50%, 65% and 80% at *station 1* are presented. It can be observed that by increasing hematocrit from 45% to 50%, the flow rate is reduced by 25%. This reduction becomes more dramatic (up to 65%) for H_t=80%. The mass flow rate reduction has a similar effect on mean blood velocity. It is obvious in Fig. 14a that the velocity is greatly reduced as H_t is increased, the reduction being, as expected, greater for H_t=80%, a fact that may lead to insufficient tissue oxygenation and progressively to tissue infarction. Moreover, low velocities may cause blood stagnation (stasis) a condition related to blood clotting and thrombosis (Stack and Berger, 2009). It can be also observed that the parabolic velocity profile flattens as the fluid becomes more viscous (Fig. 14a), a fact that is attributed to

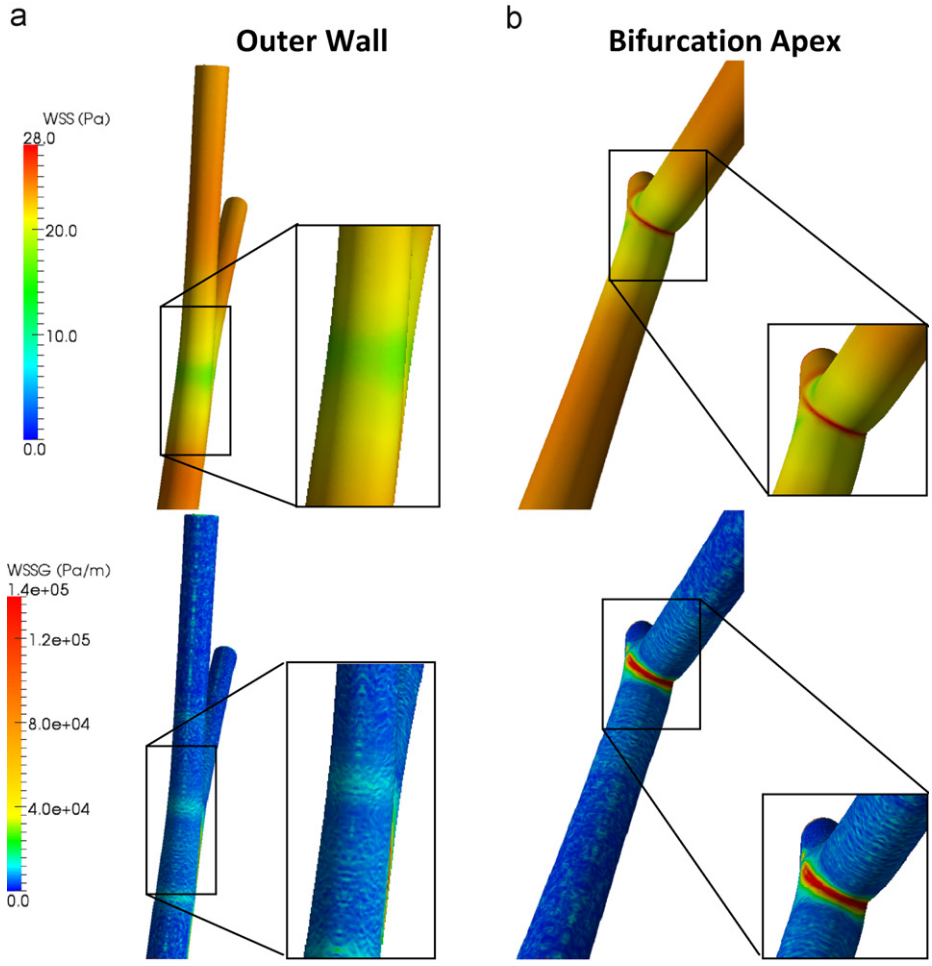

Fig. 12. *WSS* and *WSSG* on (a) the outer wall and (b) the apex of the bifurcation, for H_t=80% (*case A*, t=0.2 s).

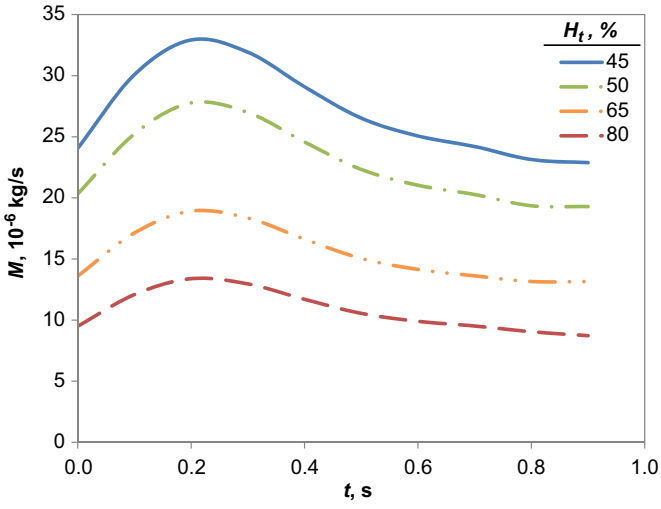

Fig. 13. Blood mass flow rate in the parent artery for various hematocrit values (*case B*).

the viscosity variation along the diameter of the blood vessel (Fig. 14b). Due to the low shear rates at the centerline of the artery, the blood viscosity attains its higher value, while closer to the walls, where shear rates are greater, viscosity tends towards its asymptotic value.

4. Conclusions

In this hemorheological study the effect of blood viscosity, expressed as a function of hematocrit, on hemodynamic factors in a small-caliber bifurcated artery was numerically investigated. This work can be regarded as an initial step towards comprehending the fluid dynamics of the blood circulatory system. It is known that blood viscosity affects the circulatory system in many ways, as it determines the value of important factors such as pressure drop, *WSS*, *WSSG*, mass flow rate and local blood velocity. In Table 2 the most important findings of this study are summarized.

The pressure drop, and consequently the pumping power needed to maintain blood flow, is proportional to viscosity. By increasing H_t from 45% to 50% both asymptotic viscosity and pressure drop increase by 14%. This implies that, in cases where the human compensative mechanisms that keep blood flow unchanged are dysfunctional, the heart must produce an additional 14% of pumping power, causing hypertension. Since the capabilities of the heart as a pump are not unlimited, by assuming that the power produced by the heart reaches an upper limit, it was estimated that for H_t=80% (asymptotic viscosity of 9.2 mPa s) the blood mass flow rate is reduced by 65%. There is evidence that individuals with high blood viscosity are more predisposed either to tissue infarction due to inefficient oxygenation, or to thrombosis due to blood clotting.

For normal hematocrit values (35–45%) *WSS* at the outer wall of the bifurcation attains low values. For the same conditions,

there is a wall region where high *WSSG* values coexist with low *WSS* ones, a condition that can lead to atherosclerosis. Moreover, the existence of high values for both *WSS* and *WSSG* on the bifurcation apex – observed for all the H_t values studied and becoming more evident as H_t increases – can affect cell alignment leading to damage of the endothelium.

Albeit the results of this study refer to two extreme cases regarding the operation of the human organism, it is believed that they can serve as an indication of the phenomena occurring in small arteries. Hemodynamic factors like pressure drop, *WSS* and *WSSG* are related to many cardiovascular diseases, and it has been proved in the present study that they are strongly associated with blood viscosity. This work provides an insight into the way that hyperviscosity may affect hypertension, atherosclerosis, blood clotting and tissue infarction. Despite the fact that viscosity is expressed here only as a function of hematocrit, it is known from limited experiments conducted in this Laboratory (Anastasiou et al., 2011) to be also greatly affected by the glucose concentration in the blood. It is reported that the high blood glucose levels can be correlated with the condition of retinal ischemia (i.e. reduced blood flow rate) developed in the course of diabetic retinopathy. Consequently, the results of this study might prove to be helpful for the understanding of diabetes effects on the blood circulatory system for patients with hyperglycemia.

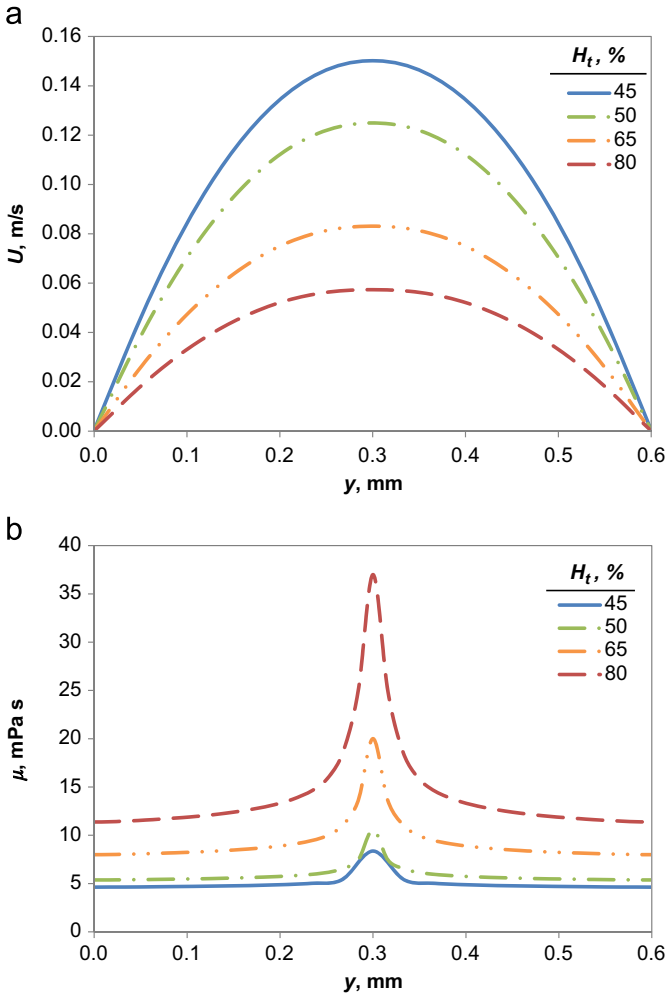

Fig. 14. (a) Axial velocity profiles and (b) blood viscosity for various hematocrit values at the parent artery for the minimum of the pulse.

Nomenclature

D	diameter of the parent artery, m
D_1,D_2	diameter of the daughter arteries, m
f	pulse frequency, Hz
H_t	hematocrit, %
H_c	critical hematocrit, %
M	mass flow rate, kg/s
m	direction vector of wall shear stress
n	direction vector normal to m and tangential to surface
n_N	asymptotic viscosity, Pa s
n_P	plasma viscosity, Pa s
P	pressure, Pa
Re	Reynolds number based on asymptotic viscosity, $Re=UD\rho/n_N$
t	time, s
U	axial velocity, m/s
U_{mean}	mean axial velocity, m/s
U_{max}	maximum axial velocity, m/s
WSS	wall shear stress, Pa
$WSSG$	wall shear stress gradient, Pa/m
y	distance from the wall, m

Greek

γ	shear rate, s^{-1}
ΔP	pressure drop, Pa mm^{-1}
μ	dynamic viscosity, Pa s
ρ	density, kg m^{-3}
τ	shear stress, Pa
τ_y	yield stress, Pa

Acknowledgments

The authors would like to thank Dr. A.A. Mouza for her critical suggestions to the manuscript.

Table 2
Overiew of the effect of high hematocrit on various hemodynamic factors.

H_t (%)	45	50		65		80	
			%		%		%
Asymptotic viscosity (mPa s)	**4.30**	4.90	*14.0*	6.90	*60.5*	9.20	*114.0*
Max axial velocity (m/s)	**0.210**	0.180	*−16.3*	0.120	*−43.3*	0.085	*−60.5*
Pressure drop (Pa/mm)	**49.0**	56.0	*14.3*	81.0	*65.3*	111.0	*126.5*
Mass flow rate (10^{-6} kg/s)	**32.9**	24.5	*−25.4*	16.6	*−49.6*	11.7	*−64.5*

- Values refer to the maximum of the pulse.
- % Difference with respect to the H_t 45% case.

References

Anastasiou, A.D., Spyrogianni, A.S., Koskinas, K.C., Giannoglou, G.D., Paras, S.V. Experimental investigation of the flow of a blood analogue fluid in a replica of a bifurcated small artery. Medical Engineering & Physics. doi:10.1016/j.medengphy.2011.07.012, in press.

Anastasiou, A.D., Spyrogianni, A.S., Giannoglou, G.D., Paras, S.V., 2011. Effect of blood viscosity on WSS of small arteries. In: Proceedings of the Eighth Panhellenic Scientific Chemical Engineering Congress, Thessaloniki, Greece, 26–28 May 2011 (in Greek).

ANSYS Inc., 2011. CFX Manual, Solver Theory, Version 13.0. Canonsburg, PA.

Çinar, Y., Demir, G., Paç, M., Çinar, A.B., 1999. Effect of hematocrit on blood pressure via hyperviscosity. Am. J. Hypertension 12, 739–743.

Chatzizisis, Y.S., Giannoglou, G.D., 2006. Pulsatile flow: a critical modulator of the natural history of atherosclerosis. Med. Hypotheses 67, 338–340.

Cuyper, M.H.M., Kasanardjo, J.S., Polak, B.C.P., 2000. Retinal blood flow changes in diabetic retinopathy measured with the Heidelberg scanning laser Doppler flowmeter. Graefe's Arch. Clin. Exp. Ophthalmol. 238, 935–941.

Dolan, J.M., Meng, H., Singh, S., Paluch, R., Kolega, J., 2011. High fluid shear stress and spatial shear stress gradients affect endothelial proliferation, survival, and alignment. Ann. Biomed. Eng. 39 (6), 1620–1631.

Farmakis, T.M., Soulis, J.V., Giannoglou, G.D., Zioupos, G.J., Louridas, G.E., 2004. Wall shear stress gradient topography in the normal left coronary arterial tree: possible implications for atherogenesis. Curr. Med. Res. Opin. 20 (5), 587–596.

John, L.C.H., 2009. Biomechanics of coronary artery and bypass graft disease: potential new approaches. Ann. Thorac. Surg. 87, 331–338.

Kitware Inc., 2011. Paraview: Parallel Visualization Application Version 3.10.1. Sandia National Labs, Los Alamos National Labs. ⟨http://paraview.org⟩.

Kroemer, K.H.E., Kroemer, H.J., Kroemer-Elbert, K.E., 2010. Engineering Physiology: Bases of Human Factors Engineering/Ergonomics, 4th ed. Springer.

Lowe, G.D.O., Lee, A.J., Rumley, A., Price, J.F., Fowkes, F.G.R., 1997. Blood viscosity and risk of cardiovascular events: the Edinburgh Artery Study. Br. J. Haematol. 96, 168–173.

Malek, A.M., Alper, S.L., Izumo, S., 1999. Hemodynamic shear stress and its role in atherosclerosis. JAMA: J. Am. Med. Assoc. 282, 2035–2042.

Merrill, E.W., 1969. Rheology of blood. Physiol. Rev. 49 (4), 863–888.

Murphy, J.B., Boyle, F.J., 2010. A Numerical methodology to fully elucidate the altered wall shear stress in a stended coronary artery. Cardiovasc. Eng. Technol. 1 (4), 256–268.

Murray, C.D., 1926. The physiological principle of minimum work applied to the angle of branching of arteries. J. Gen. Physiol. 9, 835–841.

Neofytou, P., 2004. Comparison of blood rheological models for physiological flow simulation. Biorheology 41, 693–714.

Olufsen, M.S., Peskin, C.S., Kim, W.Y., Pedersen, E.M., Nadim, A., Larsen, J., 2000. Numerical simulation and experimental validation of blood flow in arteries with structured-tree outflow conditions. Ann. Biomed. Eng. 28, 1281–1299.

Perktold, K., Rappitsch, G., 1994. Computer simulation of local blood flow and vessel mechanics in a compliant carotid artery bifurcation model. J. Biomech. 28 (7), 845–856.

Phelps, J.E., DePaola, N., 2000. Spatial variations in endothelial barrier function in disturbed flows in vitro. Am. J. Physiol. Heart Circ. Physiol. 278, 469–476.

Pries, A., Secomb, T., Gaehtgens, P., Gross, J., 1990. Blood flow in microvascular networks. experiments and simulation. Circ. Res. 67, 826–834.

Salazar-Vazquez, B.Y., Intaglietta, M., Rodríguez-Morán, M., Guerrero-Romero, F., 2006. Blood pressure and hematocrit in diabetes and the role of endothelial responses in the variability of blood viscosity. Diabetes Care 29, 1523–1528.

Shaaban, A.M., Duerinckx, A.J., 2000. Wall shear stress and early atherosclerosis: a review. Am. J. Roentgenol. 174, 1657–1665.

Shimogonya, Y., Ishikawa, T., Imai, Y., Matsuki, N., Yamaguchi, T., 2009. Can temporal fluctuation in spatial wall shear stress gradient initiate a cerebral aneurysm? A proposed novel hemodynamic index, the gradient oscillatory number (GON). J. Biomech. 42, 550–554.

Stack, S.W., Berger, S.A., 2009. The effects of high hematocrit on arterial flow—a phenomenological study of the health risk implications. Chem. Eng. Sci. 64, 4701–4706.

Tohgi, H., Yamanouchi, H., Murakami, M., Kameyama, M., 1978. Importance of the hematocrit as a risk factor in cerebral infarction. Stroke 9, 369–374.

Truskey, G.A., Yuan, F., Katz, D.F., 2004. Transport Phenomena in Biological Systems. Pearson Education Inc., New Jersey.

Woodward, M., Rumley, A., Tunstall-Pedoe, H., Lowe, G.D.O., 2003. Does sticky blood predict a sticky end? Associations of blood viscosity, haematocrit and fibrinogen with mortality in the West of Scotland. Br. J. Haematol. 122, 645–650.

Yang, X.L., Liu, Y., Yang, J.M., 2007. Fluid–structure interaction in a pulmonary arterial bifurcation. J. Biomech. 40, 2694–2699.